

On planing machine engineering characteristics and machined timber surface quality

M R Jackson*, P Hynek, and R M Parkin

Mechatronics Research Centre, Loughborough University, Loughborough, Leicestershire, UK

The manuscript was received on 28 March 2006 and was accepted after revision for publication on 4 September 2006.

DOI: 10.1243/0954408JPME100

Abstract: Rotary machined timber surfaces exhibit small waves orthogonal to the timber feed direction resulting from the intermittent engagement of the cutting tool with the timber. These surface waves are typically less than five micrometres in height and when regularly spaced at 1 mm width characterize a good quality machined surface. Variations in the regularity of these surface waves are considered as surface defects. Machined timber surfaces produced by planing and moulding machines are a typical case. These surfaces will often exhibit waviness defects caused by inaccurate contact between the tool tip and the timber being cut. There are a number of different vibration sources on these machines. The primary cause of surface waviness defects has been found to be forced vibration, although inaccurate cutter servicing and relocation are also factors. The work presented in this paper concentrates on phenomena caused primarily by forced structural vibration. Systematic engineering and wood machining investigations are applied to a special purpose instrumented test rig so that correlation between vibration data and observed waviness defects can be established. The surface assessment of machined timber is carried out using a special purpose contact based surface tracing instrument. The engineering design and manufacturing influences that lead to unacceptable surface waviness variation effects are discussed.

Keywords: waviness, surface finish, forced vibration, wood

1 INTRODUCTION

Planing and moulding machines for timber processing are widely used in manufacturing industries. These multi-spindle high-speed machines are in most cases required to produce machined timber quality with a surface wave height h of less than 5 μm . Each high-speed ($n = 6000$ r/min) rotating spindle unit may employ a cutterhead with typically $N = 4-8$ cutters producing a cutterhead/spindle assembly mass of 15 kg. On high-speed planing machines, a timber feed velocity $V = 200$ m/min is possible with up to 20 cutters in a 30 kg cutterhead. This combination of multiple high-speed and relatively large mass rotating systems mounted on a common structure provides scenarios for forced

vibration that can easily produce machined timber surface quality degradation.

The commercial impact of machine-induced waviness defects is complicated by machine user and also trade/public perception of what is required of a timber surface. There is only very limited standard information on timber surface quality and this does not include waviness variation quality. The quality aimed for is dependent on end usage, yet the planing and moulding machine needs to be capable of producing work of the best quality with little skill on the part of the labour force. A review of timber planing and moulding machine history is provided in reference [1] with a substantial reference list, including relevant metal machining references from both milling and grinding fields of research.

The aim of this paper is to extend the work presented in reference [1] that deals with simulation of two classical surface degradation mechanisms widely observed in the timber processing industry. The extent to which these phenomena are considered a surface defect

*Corresponding author: Wolfson School of Mechanical Engineering, University of Loughborough, Loughborough, Leicestershire LE11 3TU, UK. email: m.r.jackson@lboro.ac.uk

depends entirely on the perception of both the machine user and timber product consumer. It is often the case that a planing machine manufacturer will be called to investigate a surface finish problem that has suddenly arisen on a machine that has apparently been performing satisfactorily since commissioning. The explanation of the sudden occurrence of a fault can, in many cases, be explained by the fact that there has been a change in the level of timber surface quality discernment by the machine user and/or receiving product client. This leads to the perception that the machine has suddenly malfunctioned in some way. A similar situation occurs when an operator is changed on a machine that apparently has worked well for years. This is because an experienced operator will have coaxed the necessary performance from a machine in order to achieve acceptable surface quality. This operator knowledge and skill are not documented and often the operator does not fully understand precisely what has been done to achieve the desired quality. This is the 'black art' of the process and is not unusual in some manufacturing industries. Such cases of apparent product malfunction are not rare and significantly distract engineering staff at both the machine builder and machine user companies.

This paper presents results of a detailed process study on a test facility developed to represent a real industrial timber machining process. The test rig is instrumented with displacement and accelerometer sensors. The test rig is adaptable to enable structured engineering changes to be implemented in order to determine their influence on machine vibration signatures and the measured surface waviness of machined timber samples.

It is the belief of the authors that this paper will provide technical insight as well as engineering realization understanding to aid future process research and development. This information is based on the unique research and engineering experience of the authors in the European Union woodworking machine tool industry applied in world wide markets.

2 RELEVANT LITERATURE

The literature cited in this paper will be limited to the field of woodworking research. There are associated references from the metal machining community, in particular milling and surface grinding as detailed in reference [1].

Waviness phenomena on timber surfaces were first reported by Petter [2] in the 1950s. Subsequent work by Mori and Hoshi [3–5] in the 1960s compared experimentally observed wave width variation with theoretical predictions to aid understanding of the physical phenomena. Other work by Koch [6, 7] dealt primarily with the machining kinematics and

subsequent cutting action to form different chip types producing the corresponding surface texture quality on the machined timber samples. Kivimaa [8] examined cutting forces in woodworking in 1952. Despite being over 50 years ago this remains the only piece of substantial work on cutting forces generated for rotary machining of timber. In comparison with instrumentation technology available today, Kivimaa's method of force measurement based on springs and displacement gauges is considered primitive, but at the time was the only solution. The extent to which Kivimaa's cutting force data are considered accurate is not formally reported. Salze (1978, Personal Communication) reports cutting forces measured with modern instrumentation applied in a rotating cutterhead. Work by Jackson [9] examined cutting forces in some detail using a 3-axis quartz dynamometer but only for a specific case of softwood machining with a sharp cutting tool and also for a jointed cutting tool. (Jointing is the term used to describe cutting tool dressing at the operating speed to true all cutters to a common cutting circle so improving surface quality at increased feed speed [1].) Interestingly, both of these works report cutting forces of a similar order of magnitude to Kivimaa.

In the 1980s, Jackson [10] investigated waviness generation and possible solutions. This work was carried out at a major manufacturer of machine tools in the UK. More recently Heisel and Krondorfer [11] in 1992 investigated forced vibration generating specific cases on a modified spindle unit.

2.1 Surface waviness variation

Work reported in reference [1] summarizes the industry considered view for typical waviness values on perfect machined surfaces. The vertical amplitudes of perfect surface waves for good quality surfaces as predicted by theory are: – furniture 2 μm , joinery 5 μm , sawmilling 8 μm – although sawmilling can be similar to joinery in higher quality sawmilling production. A special case of sawmilling type manufacture is the production of high quality strip mouldings (or profiles) that require furniture quality machined surfaces (e.g. for picture frames).

Furniture and joinery work are normally carried out with a single knife finish technique as described in reference [1]. The primary cause of surface defects in this case is drive motor vibration or structural resonances at frequencies other than the spindle rotational frequency. This case is not examined further in this paper.

A second type of waviness defect occurs when the jointing process is applied in sawmilling [1]. This type of machined surface exhibits a once per cutterhead revolution effect (1/rev) that can be caused by

one proud knife or by eccentric running of the cutterhead relative to the machined timber surface. Depending on the severity of this once per revolution effect, a waviness defect on the machined timber surface will be classified (Fig. 1). Investigation of causes and solutions to this once per revolution effect is the focus of this paper.

Sawmilling work is normally carried out at the higher timber feed velocities, typically 50–150 m/min. This process requires the jointing technique to be applied to achieve the high speeds involved. Ensuring an acceptable waviness quality under these conditions is the motivation for the work reported here. Table 1 shows data for 1/rev surface waviness variation defects in the case where jointing of the cutters is applied to a four knife cutterhead with a cutting circle of 130 mm diameter. (Cutting circle is the diameter of the cutter tips.) This is compiled from references and confirmed by the authors' research and industrial experience.

A range of wave pitches are aimed for during production of sawmilling products (mouldings, skirting, architrave, tongue and grooved boarding, cladding). A wave pitch of 1.75 mm is considered at the lower quality level whereas a wave pitch of 1.25 mm is at the higher quality level with 1.5 mm being the middle quality level. These are shown in Table 1. Also shown in the table are the ratios of wave width for each nominal wave pitch subjected to a modelled interference at $a_{1/rev}$ (theory reported in reference [1]). The ratios of $R_w (= W_{min}/W_{max})$ and W_{min}/p are presented. (The wave height ratio reported in reference [1] has not been tabulated.) The former based on min/max wave width variation and the latter on the basis of adjacent wave width variation. Both of these ratios are set to 0.7 based on practical observation from industrial quality assessments carried out by the authors. For a given value of 0.7, the corresponding values for $a_{1/rev}$ can be calculated

[1]. From Table 1, $a_{1/rev}$ values based on $R_w = 0.7$ are always less than those calculated for the $W_{min}/p = 0.7$ ratio. $a_{1/rev}$ based on the former is typically 0.6 times $a_{1/rev}$ calculated for the latter case. This is logical since to get an adjacent wave width variation of 0.7, the amplitude of $a_{1/rev}$ must be greater. Which method of assessment should be used is not established. For the case where $R_w = 0.7$ is used as the desired limit of wave width variation in Table 1, the range of $a_{1/rev}$ across the quality range for sawmilling is determined as nominally 4–2 μm . Using the limits of $W_{min}/p = 0.7$ results in $a_{1/rev}$ ranging nominally from 7–3.5 μm . Both cases are an exacting requirement for any planing and moulding machines. These levels of quality are often met for the $W_{min}/p = 0.7$ case, but often not for the $R_w = 0.7$ case, mainly due to variation in machine state and tooling set up.

Increased numbers of cutters for higher feed speeds result in larger cutterhead radii and hence shallower wave heights for a given pitch [1]. The larger radius and reduced wave height initially lead to the conclusion that this type of machining condition will be more sensitive to displacements normal to the surface. Although this is true for each cutter position, the influence of $a_{1/rev}$ is actually reduced because as the number of cutters increases the linear distance between the high and low points of the waviness cycle on the timber surface also increases and consequently the 1/rev waviness defect is less obvious. Older machinery (circa 1950s) used lower spindle speeds (3000 r/min) and increased number of cutters (10–12) mainly because of concerns on vibration due to tooling imbalance and also tooling strength. Latterly, the modern trend is towards higher spindle speeds (6000 r/min) and less cutters to reduce tooling costs and set up times. This places the machining operation in a region where $a_{1/rev}$ can substantially affect waviness quality on a four or six knife cutterhead. Understanding how to make this four or six knife high rotational speed operating condition robust is at the centre of the work reported here.

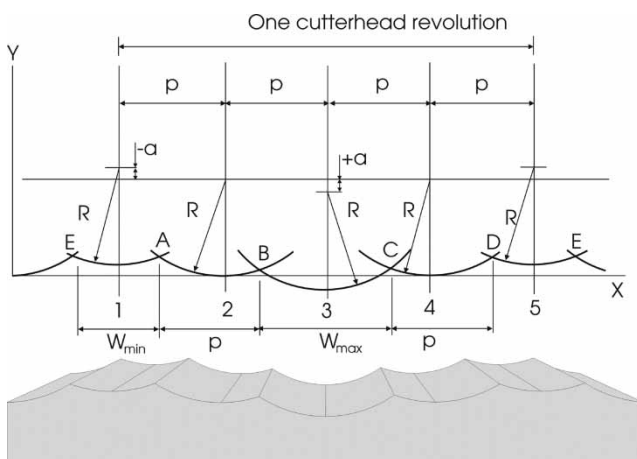


Fig. 1 4 Kn Finish 1/rev waviness defect

2.2 Cutting forces

Figure 2 shows cutting force directions relative to cutterhead and timber movement. The tangential force (F_t) is generally associated with the rotational effort (torque) to cut the timber and is typically 4 N/mm for a depth of cut of 0.5 mm in softwood with 12 per cent moisture content cutting parallel to the timber grain using a work sharp cutter. (Work sharp means newly sharpened cutter which has cut only a few metres of timber.) The corresponding peak levels of normal force (F_n) are typically 1 N/mm width of cut. The observed tangential and normal force characteristics were first identified

Table 1 Wave width ratios for 1/rev defect case–4 knife finish

$R = 65 \text{ mm}$	$R_w = 0.7$	$W_{\min}/p = 0.7$	$R_w = 0.7$	$W_{\min}/p = 0.7$	$R_w = 0.7$	$W_{\min}/p = 0.7$
$p \text{ (mm)}$	1.75	1.75	1.5	1.5	1.25	1.25
$a_{1/\text{rev}} \text{ (}\mu\text{m)}$	4.16	7.07	3.05	5.19	2.12	3.61
$W_{\min} \text{ (mm)}$	1.44	1.23	1.24	1.05	1.03	0.88
$W_{\max} \text{ (mm)}$	2.06	2.28	1.76	1.95	1.47	1.63

by Kivimaa [8]. Later work (J. Salz, 1978, personal communication) [9, 10] supports these observations for the limited case of planing timber. Normal forces are of interest in this work because they may affect the cutter locus during the initial phase of the cut which forms the resultant machined timber surface (for up-milling). (Up-milling is used on most woodworking machines instead of climb milling due to workpiece feed safety considerations.) Figure 3 shows a typical normal force trace from reference [9], obtained at one-sixth operating speed and measured using a quartz dynamometer and oscilloscope instrumentation. By convention, positive normal cutting forces are defined as those which push the cutter tip and timber apart. Negative forces pull the timber and cutter together. By consideration of Figs 2 and 3, it can be postulated (with some confidence) that the initial stage of the cut is essentially a rubbing action where the cutter (supported by a compliant spindle) is exerting pressure on the compliant timber surface until such time as the cutter ‘digs into’ the timber and starts to form a chip. This idea has been presented without clear evidence (simply limited by instrumentation) by both Koch [6, 7] and Kivimaa [8]. In Fig. 3, the proportion of the total cutter engagement time with the timber that is positive indicates the rubbing region. This normal cutting force waveform can be scaled against the calculated path length of the tool tip engagement with the timber (L) and thus

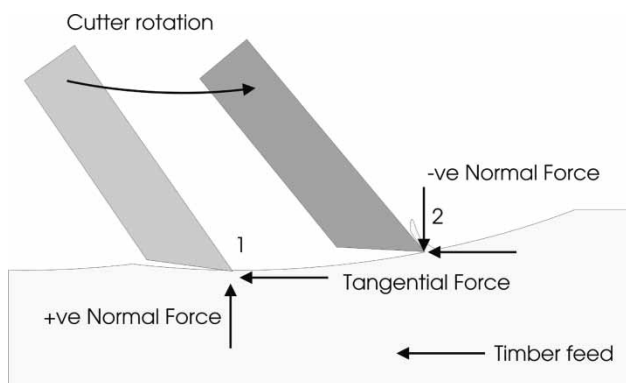


Fig. 2 Normal and tangential cutting forces during rotary machining of timber
Note: cutting force arrows represent force on tool tip

determine the length of the positive rubbing region and the negative cutting region. The proportion of rubbing and cutting changes with tool geometry and machine settings (and probably machine dynamic characteristics). For the waveform shown in Fig. 3 with $p = 1.5 \text{ mm}$ and calculated cutting path length $L = 8.78 \text{ mm}$, the rubbing region extends to 3.1 mm , i.e. twice the finished wave width p . Figure 3 provides clear evidence that the surface wave is formed during the rubbing phase of the rub-cut cycle. Koch [6, 7] indicates that this may be a machining operation based on a type 1 chip where the timber crumbles into a powder rather than producing a real (severed) type 3 chip. (See references [6, 7] for a fuller explanation of type 1, 2, and 3 wood chip formation.) Larger wave pitches and increased depth of cut reduce the positive region – i.e. less rubbing occurs, replaced by a longer cutting region.

Normal forces are further increased by the jointing process. The circumferential joint land formed by the jointing process as it trues the cutters to a common cutting circle in effect removes the back clearance angle γ as well as increasing the tip sharpness angle β from 40° to 60° . Both of these changes further promote rubbing.

Understanding what happens in this rubbing region so that the effect on surface waviness (and texture) can be more fully understood is key to controlling surface finish, tool wear, and power consumption. Figure 4 shows how the normal force changes with increasing joint land width. The forces are reported as peak–peak. In actual fact, when jointing is applied, these forces are entirely positive for the surface generation part of the cutting cycle, i.e. the rubbing condition applies. The relationship between joint land and normal cutting force as the joint land width increases from sharp (land = 0) to 0.5 mm (normal industrial limit) is clear. These data show that a joint land width of 0.3 mm will generate twice the value of normal force as a joint land width of 0.1 mm . The relationship is clearly non-linear but also becoming less sensitive as joint land width increases. Joint land width and normal forces need to be considered in any future analysis simply because each cutter in the cutterhead will have a land width dependent on tool grinding results, relocation eccentricities on

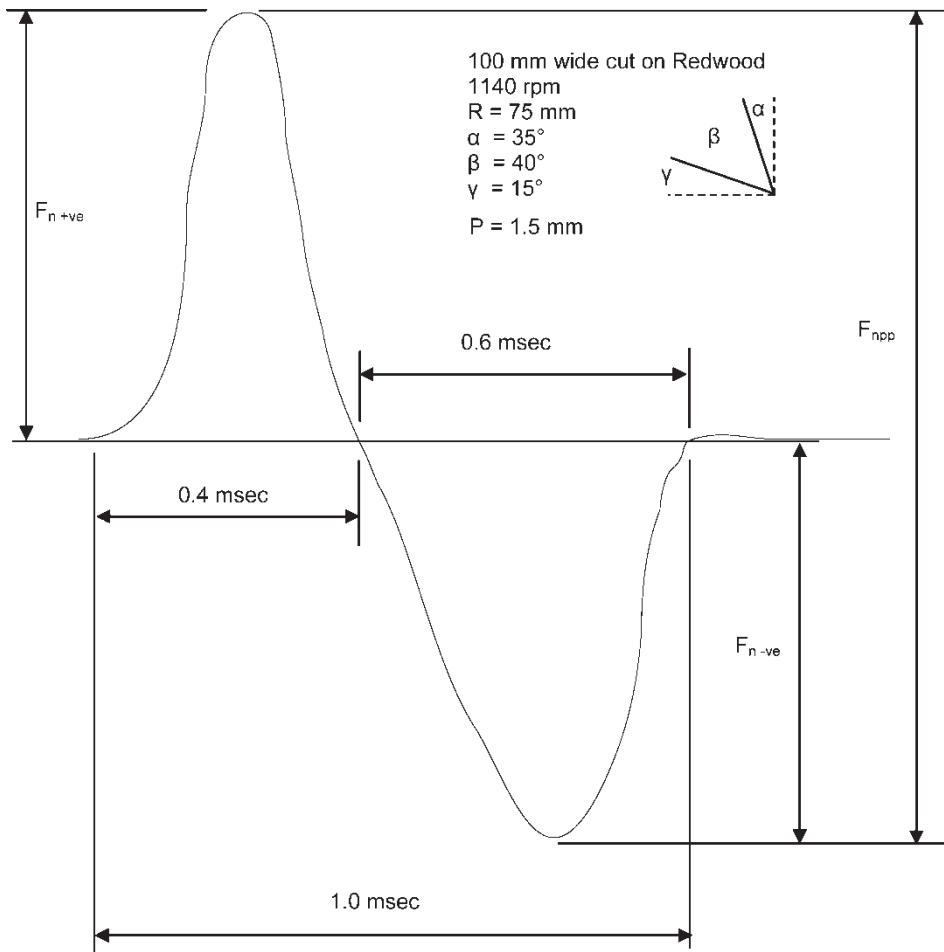


Fig. 3 Typical normal force waveform

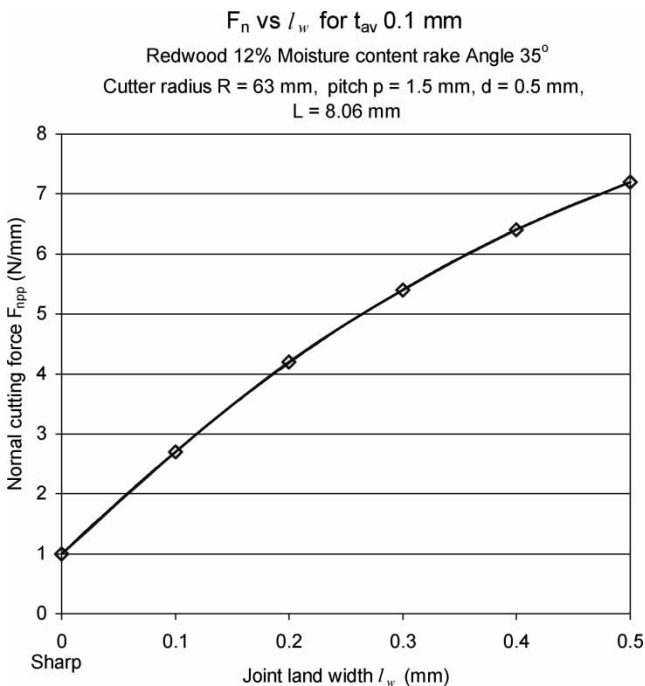


Fig. 4 Effect of jointing on normal cutting force F_n

the planing machine spindle, and any vibration present during the jointing process. The resulting joint land variation cutter to cutter will produce a corresponding normal force variation and potentially different tool tip loci through the timber. This may cause variation in surface wave heights and widths. For this reason, it is essential to measure joint land width during machine performance testing.

3 FORCED VIBRATION

The major mechanism that produces surface waviness variation on machined timber is that of forced vibration. This is unlike milling of metals where 'chatter', i.e. instability is in the main structure and drive systems are a major cause of surface waviness defects, although forced vibration also produces surface defects in milling of metals. Forced vibration can also influence the surface waviness of precision ground metal components [9]. A further mechanism for surface waviness defect generation is due to misaligned spindle bearings that produce a twice

per revolution vibration that reproduces on the machined timber surface. Superficially, this surface defect on a four knife jointed cutterhead seems the same as for case 1 [1] where a 1/rev interfering forced vibration at half the spindle speed in single knife finish machining conditions produces a light-heavy-light-heavy wave pattern on the timber surface. However, the engineering procedure to provide a solution is different for each case. In the case of twice per revolution vibration, the bearings need to be aligned correctly and in the once per two revolutions case, the forcing frequency from the half spindle speed drive motor needs to be removed from the cutter spindle via motor/pulley balancing, dynamic isolation, or structural characteristic modification or a combination of these solutions.

Cutting forces generated when machining timber occur at high frequencies (5 kHz is typical). Therefore, the forces applied to the machine structure are correspondingly small and do not normally induce chatter generation and corresponding surface defects. With timber surfaces, the degradation takes the form of width/height modulation of surface waves resulting on the timber from the rotary machining action modified by a combination of forced vibration and tool sharpening errors.

This paper is concerned with forced vibration of a four knife jointed cutterhead where the major vibration component is due to spindle rotational frequency, usually caused by imbalance and structural deflection. The frequency range of interest, associated with typical industrial applications is 75–400 Hz. The lower value of 75 Hz corresponds to a rotational speed of 4500 r/min, whereas 400 Hz corresponds to a 6000 r/min spindle speed (100 Hz) multiplied by the number of cutters in the cutterhead – four in this case. The cutter passing frequency must be considered because of the possibility of subtle cutting force effects (not chatter). It is not normal practise to joint cutterheads above 6000 r/min spindle speeds, although there is no clear technical evidence for this limit [9].

It is possible to dynamically model the broad effects of forced vibration. The cutterhead and spindle assembly stiffness are assumed to be infinite, i.e. the variables for support stiffness include both spindle bearing and support structure stiffness. Typical modelling activity based on classical equations can be undertaken in MATLAB[®]. Detailed reportage is the subject of a future paper. The results of such modelling correspond closely to practically identified cutterhead natural frequencies (by impulse method and variable speed method). It is clear that major resonances occur within the operating range of these types of woodworking machines. This is not unusual in industrial equipment of this general size. Given this, it is entirely possible for the slight

imbalance due to the small endemic eccentric rotation of a heavy cutterhead to generate significant forces. Typical forces at the spindle speed of 6000 r/min and cutterhead mass of 15 kg are ± 12 N at 100 Hz. While these forces are not high, the support stiffness values of typically 30 N/ μm mean that ± 2.5 μm are possible just based on static calculations. In practise, the values can be greater than this due to resonance effects.

Eccentric running of the cutterhead spindle comprises of two parts: static eccentricity due to minor imperfections in component manufacture and dynamic eccentricity at the operating speed resulting from spindle/cutterhead imbalance interacting with support structure flexibility. Imbalance also comprises of two components: due to static eccentricity of the cutterhead mass, and imbalance forces due to any further eccentricity increase due to the flexible nature of the support structure and rolling element bearing system. These imbalance components combine to produce a rotational speed sensitive dynamic eccentricity initiated by static imbalance that interacts with support system compliance, thus, producing increasing eccentricity with rotational speed.

Depending on the position of the jointing device, this dynamic eccentricity and also the static eccentricity of the cutters can be dressed out. Due to cutter grinding off the planer moulder and subsequent relocation on the cutterhead spindle. This has been the premise of the jointing approach for the past 50 years. For machining conditions at the lower quality end of the market, this has indeed worked. As timber machining companies try to expand (or indeed retain) their markets by improving quality, the existing process shows up once per revolution surface waviness modulation effects that are often considered defects. Purists would have the jointing device located at the point of cutting to be sure that all eccentricities are removed at the cutting point, but this is not practical. More usually jointing devices are located at either the 11 o'clock or 2 o'clock positions when viewed from the front of a horizontal top head as shown in Figs 5 and 6. Concerns about these locations exist because it is postulated that non-circular cutterhead orbits will generate a jointed shape on the cutters that does not compensate the initial inaccuracies of cutter tracking resulting from the cutter grinding and relocation on the machine spindle. Furthermore, in some cases, the jointing device itself can modify the jointed cutter tracking orbit due to jointer vibration excited by cutterhead imbalance (the jointer behaves like a cam grinding device) or by modifying structural dynamics and thus influencing spindle orbit – in the case of removable jointing devices for example.

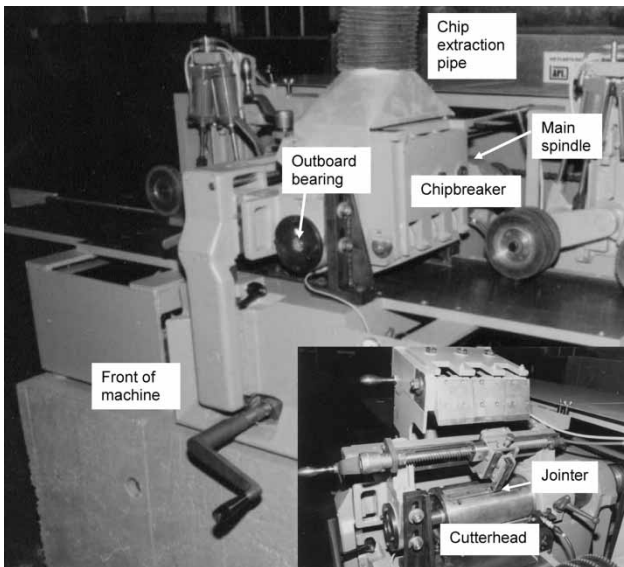


Fig. 5 Test rig for planing investigation

The random nature of these tooling and machinery induced cutter tracking modifications from the point when the machinery is first assembled and also during service life, subtly change the machining performance of very expensive and heavy machinery (typically 10 tonnes), where the sole design purpose of these machines is to produce high-quality machined surfaces.

To investigate these effects, a special purpose test rig was designed based on a top head unit of a high-speed planing and moulding machine. This head had variable performance in industry and thus was a good candidate for systematic investigation and modification for improvement of machining quality.

4 EXPERIMENTAL FACILITY

The special purpose test rig used for engineering and wood machining investigations is shown in Fig. 5. The test rig comprises of a main spindle unit and drive motor, integrated timber feed rollers (feeding timber from right to left) located on a one tonne steel reinforced concrete base. The base was mounted on a machine tool foundation via industrial anti-vibration mounts.

At a main spindle speed of 4350 r/min, four knife jointed operation, and the integrated timber feed-works set at the following speeds (measured on the timber surface), the corresponding cuttermark widths are:

- 36 m/min = 2.0 mm wave pitch
- 26 m/min = 1.5 mm wave pitch
- 17 m/min = 1.0 mm wave pitch

Careful design and benchmarking with a full production machine confirmed that this test rig gave representative performance. Figure 7 shows a cross-sectioned view of the top head structure of the test rig. The main spindle housing is shown behind the fence line (FS) timber guide. This spindle housing incorporates a super precision ball bearing pair in back to back configuration. Outer race diameter is 100 mm. The outboard bearing housing located on the left side of the arrangement at the near side (NS) incorporates a single row super precision deep groove design of 85 mm outer race diameter. A Tufnol sleeve is located inside the bearing inner ring. The cutterhead spindle locates in the bore of the Tufnol sleeve. This arrangement provides a run time support for the cutterhead spindle. The Tufnol sleeve is keyed to the cutterhead spindle. The outboard bearing housing is removed

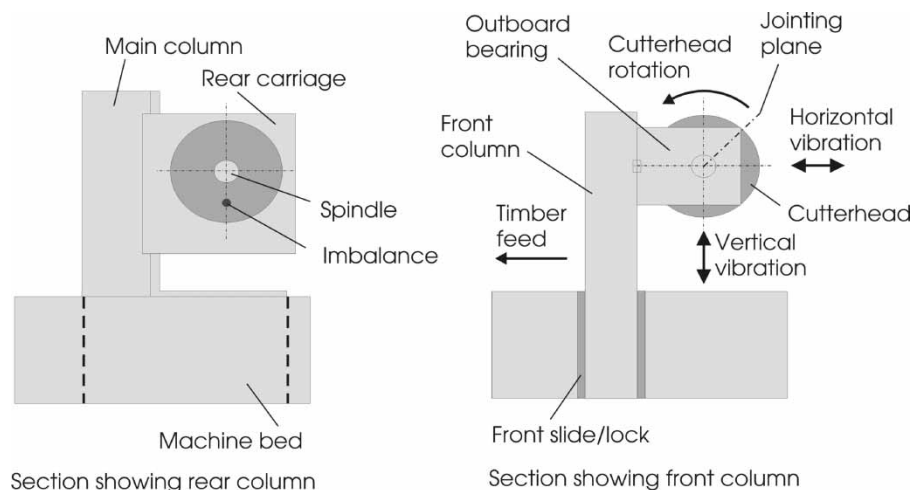


Fig. 6 Standard structure – front view

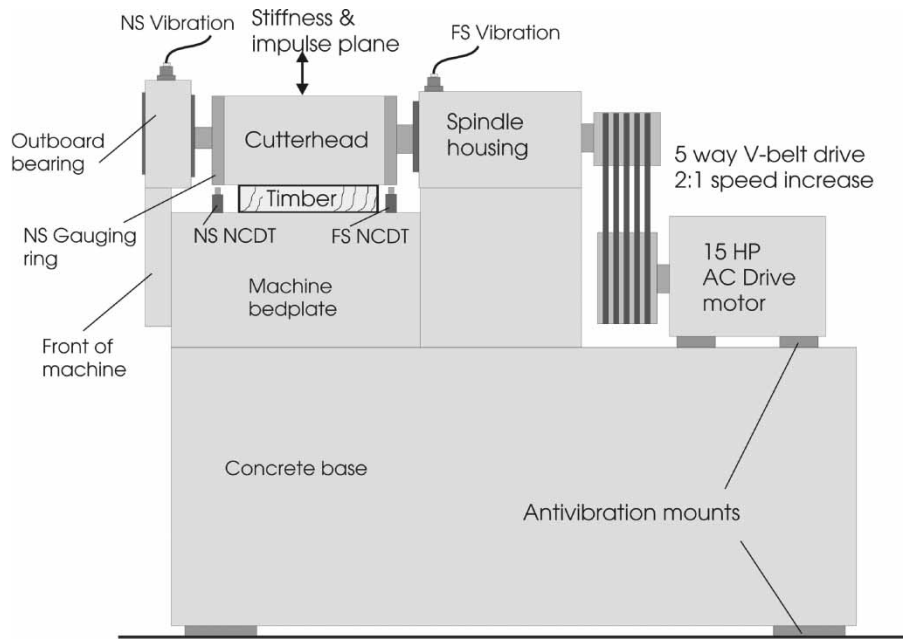


Fig. 7 Test rig arrangement – view in timber feed direction

by releasing a lock nut when cutterhead removal is required. The extra support from the outboard bearing allows cutter jointing to be carried out to improve timber surface quality at higher feed speeds. The fit of the spindle in the Tufnol sleeve is H7-g6 (close location fit), this can introduce a diametrical clearance of 5–90 μm theoretically. In practice, the limits are controlled by selection to produce 5–25 μm .

The jointing device is of the removable type. To use the jointer, the chipbreaker unit has to be raised, then the jointer is clamped in position (Fig. 5). These two actions significantly alter the dynamics of the standard machine structure.

Initial static stiffness measurements at the FS and NS of the structure showed the FS to be 105 $\text{N}/\mu\text{m}$ with the NS (outboard bearing side) 30 $\text{N}/\mu\text{m}$. The lower stiffness at the NS may well be due in part to the clearance fit between the Tufnol sleeve bore and the cutterhead spindle. The stiffness graphs do not indicate a classic non-linearity when the clearance is traversed. It is thought that assembly misalignments effectively linearize this effect. The other contributors to low stiffness at the NS are deflection of the supporting structure as well as the internal clearance of the deep groove outboard bearing. Both of these are secondary to the effect due to the Tufnol sleeve. While the overall machine construction seems adequate for planing timber, it is clear that subtle detail differences exist at the interfaces between critical components.

The standard type of cutterhead for this machine would have originally been mechanical collett and

cone location based. This system allows the cutterhead to be centred on the spindle within certain broad limits. From experiments the degree of cutterhead eccentricity resulting from this centering approach is within the range 5–75 μm . This range is determined by the eccentricity of the spindle, the eccentricity of the cone in the cutterhead and the eccentricity of the cone on the collett. By rotating the phase angle of each element eccentricity the 5–75 μm range can be obtained. The cutterhead diameter is 145 mm with a mass of 10 kg, thus a maximum imbalance due to the cone and collett location system is 750 $\text{gm} \cdot \text{mm}$, considering static imbalance. While machine designers had introduced this cone and collett system in the 1950s, in actual fact a more reliable (but possibly on average more inferior) result could have been achieved with a plain H7-g6 location fit. There is no evidence that the collets were used to find the best point of smooth running. Usually, operators just reported degradation of machined surface quality, when unfavourable balance conditions resulted from random relocation of these eccentric components. In the light of this experience and analysis, the cutterhead on the test rig was modified to include two hydraulically contracting bushes (known as Hydrogrip bushes) to improve centering ability to within 5–10 μm . The effects of the cone and collett system were simulated (approximately) by addition of imbalance masses. The cutterhead was also modified to include gauging rings at each end so that non-contacting displacement transducers (NCDT) (capacitive type from Wayne Kerr) could be used to

measure spindle and cutterhead orbit. The location of these NCDTs at both the NS and FS positions is shown in Fig. 7. The NCDTs were located to measure both vertical (as shown) and horizontal (not shown) during the initial investigations.

Accelerometers from Bruel and Kæjr were used to gather structural vibration data at the key points around the main spindle, outboard bearing and also the machine bedplate and the one Tonne concrete base. The latter was custom made with steel reinforcement to add substantially more mass so that the support structure did not degrade the machining performance of the test rig. All signals were analysed using a Spectral Dynamics real-time Fourier spectrum analyser. The cutterhead was two plane dynamically balance *in-situ* to reduce imbalance to a minimum of 50 gm · mm. A 10 KW AC motor drives the main spindle via a 2:1 stepup five-way V-belt transmission system. A commercial frequency inverter is used to vary the motor spindle speed within the range 1500–6000 r/min. Timber softwood samples were machined for each key stage of the test rig refinement. The cutting width of the cutterhead is 250 mm. The surface waviness of each test sample of timber was measured immediately after machining using the waviness recording instrument (WRI) detailed in reference [1].

5 EXPERIMENTAL WORK

The method for the experimental work carried out on the test rig described in section 4.0 is as follows.

5.1 Engineering tests

1. Physical misalignment of the outboard bearing unit relative to the spindle centre in the vertical and horizontal planes establishes the effect on spindle orbit and structural acceleration.
2. Impulse testing of the structure at key positions using the spectral dynamics real-time Fourier spectrum analyser. These key positions are the vertical direction at the centre of the cutterhead cutting width (Fig. 6) and the vertical and horizontal directions on the main spindle and outboard bearing structures, as shown in Fig. 6.
3. Static stiffness measurements of the cutterhead relative to the machine bedplates in the vertical plane were taken with a centrally applied preload equal to the cutterhead weight (100 N) and incrementing a centrally applied upwards load from zero to twice the cutterhead mass (i.e. 200 N). This is a standard machine tool stiffness assessment method.
4. Sweep speed testing between spindle speeds of 1500–6000 r/min to detect any resonances. The

spindle speed was incremented in 500 r/min steps but also finely adjusted around speeds where resonance occurred. The spindle speed was held constant for a duration of 30 s at each sweep point. The average NCDT value was recorded. There was approximately 5 per cent fluctuation in NCDT signal levels at each speed throughout the range. Any sweep detected resonances were checked against possible resonances detected in the impulse tests. The severity of acceleration on the test rig structure as well as the displacements at the NCDT positions to determine cutterhead orbit were measured for each speed increment. The sweep test was carried out with zero imbalance and high imbalance (675 gm·mm) – the latter was applied at the four discreet positions in the NS gauging ring at the same angular position as each cutter in the cutterhead. Zero imbalance is that due to 2-plane balancing of the cutterhead and cutters *in-situ* ~50 gm · mm.

5.2 Woodmachining tests

The wood machining tests were carried out on Scandinavian Redwood with a moisture content of 12–14 per cent. The timber sections were planed to a rectangular section just prior to carrying out each of the cutting tests. The samples were 180 mm wide and between 30 and 50 mm thick and 1.5 m in length. The general test procedure is outlined below with further detail in Table 2.

1. The cutters were sharpened in the four knife cutterhead by means of a straight knife grinder. Cutter run out on grinder arbour was within the range 5–10 μm as measured by a 0.001 mm dial test indicator (DTI). Note that this is total indicator reading (TIR) so eccentricity is half of these values (i.e. 5–10 μm TIR is 2–5 μm eccentricity). The cutterhead was transferred to the test rig spindle and the outboard bearing locked in place. The cutterhead hydraulic sleeves were pressurized to 650 bar by means of a grease gun. The cutter run out (TIR) was within the range 10–20 μm .
2. A 0.5 mm depth of cut was taken on each test. This is typical of a finishing planing operation. There was no reduction in spindle rotational speed during the idling to cutting phase.
3. The cutterhead was rotated at the desired speed – standard was 4350 r/min. Structural acceleration and cutterhead orbit peak–peak displacements were measured at key positions – the minimum number of measurement points were as shown in Fig. 7 (i.e. vertical NS + FS).
4. The spindle was stopped. The chipbreaker raised and the jointer clamped in position (Fig. 5). The

Table 2 Experimental tests – measured parameters

Parameter	Comments
Structural displacement and cutterhead orbit at NS, FS vertical and horizontal directions for a range of operating speeds	Accelerometers placed on machine structure to confirm any structural displacements in relation to cutterhead orbit relative to machine bed measured by NCDTs
Radial stiffness of cutterhead normal to plane of timber surface	Static measurement via centrally applied load and measurement of cutterhead displacement at FS and NS positions using embedded NCDTs
Natural frequency of cutterhead and bearing assembly	Static impulse method: to determine how structural modifications affect this parameter
Cutterhead orbit (jointing phase) [$B - J_1$, $C - J_2$]	To detect any orbit differences between the cutting (B, C) and jointing plane
Static jointed cutter tracking	To indicate results of jointing process and confirm any relative radial displacement between jointing stone and cutter
Cutterhead orbit (cutting phase) [$B - B_c$, $C - C_c$]	To detect any changes in spindle orbit between jointing and cutting phase
Surface waviness pitch and height data ($p = 1.5$ mm)	To confirm the resulting machined wood surface waviness pitch, height and variation

All of the above measured for standard structure, Stage 1 and Stage 2 modified structures.

spindle was started again to run at the operating speed. Jointing was carried out. It was also possible to measure the cutterhead gauging ring displacement relative to the jointer in the jointing plane at both the FS and NS positions. This was done using a separate NCDT mounted on the jointer carriage.

- When jointing was judged to have occurred on all four cutters, the spindle was stopped and the static cutter run outs measured at both FS and NS positions. The joint land width was measured using an eyepiece with graticule of 0.1 mm graduation.
- After jointing, the chipbreaker was lowered and the spindle was run at the desired cutting speed (normally the same as the speed at which jointing was carried out). A test cut at the set feed speed was then carried out. A typical time for signal acquisition was 3 s. Longer pieces of timber were used to provide longer acquisition times as required. Vibration levels during cutting were also recorded via the Spectral Dynamics real-time Fourier spectrum analyser.
- The surface waviness of the machined timber samples was measured using the WRI.

The above test programs were implemented for the standard machine arrangement (standard structure Fig. 6), a stiffer structure implemented by stiffening elements at both the FS and NS, including additional outboard bearing slide clamps (Stage 1 modification as shown in Fig. 8) and a further modification to remove the Tufnol sleeve clearance with the spindle by means of a substitute hydraulically contracting sleeve (Stage 2 modification shown in Fig. 9). It should be noted that Stage 2 comprises of the structural stiffening elements of Stage 1 plus the hydraulically contracting sleeve shown in Fig. 9.

6 TEST RESULTS AND ANALYSIS

A large amount of test data have been obtained from this test work. A selection is presented here in Tables 3 to 5 and Figs 7 to 13 to show the key findings of the research.

6.1 Engineering test results

A preliminary vibration assessment of the test rig showed that the rigid body mode vibration of the machine concrete base and bedplate section was two orders of magnitude lower than the main spindle support structure vibration. There was no frequency component associated with the main drive motors (spindle and feedworks). There was no vibration beating due to the V-belt drives.

6.1.1 Misalignment investigation results

During the initial vibration survey, it was discovered that the normal fitment dual rise and fall leadscrew arrangement (one at the FS and one at the NS linked by a common actuation shaft) for the spindle

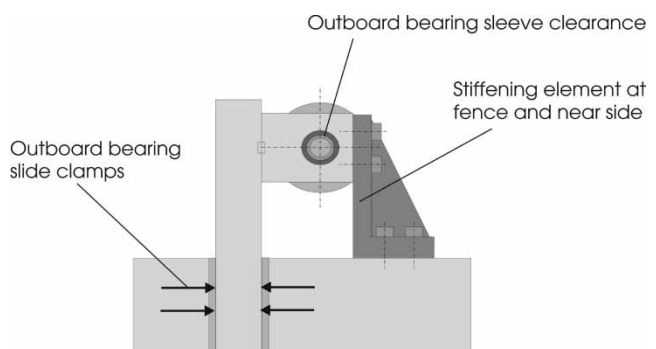


Fig. 8 Stage 1 modification – front view

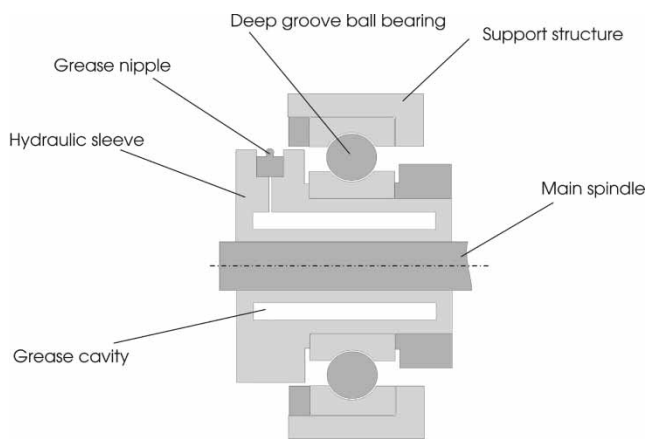


Fig. 9 Stage 2 modification

support structure unit could easily introduce $30\ \mu\text{m}$ uncertainty in standard structure outboard bearing main spindle alignment due to friction in the front/rear slideway/screw adjustment design. This results in variable amounts of outboard bearing misalignment with the main spindle.

The outboard bearing was incrementally adjusted from the as manufactured position (denoted as '0' to $\pm 120\ \mu\text{m}$ in the vertical direction. This test was done to establish if any misalignment was present. At a position that was $40\ \mu\text{m}$ below the '0' position, the NCDT amplitude at the spindle frequency n at the NS reached a maximum of $45\ \mu\text{m}$ pp and $2n$ amplitude at a minimum of $4\ \mu\text{m}$ pp. pp is peak-peak for all NCDT values – eccentricity is half peak-peak. This indicates the point where best alignment occurs. This minimizes the $2n$ interference but allows maximum n amplitudes to occur. This might be expected since the effect of misalignment is to preload the main spindle and thus reduce or remove the internal clearance of the outboard bearing and Tufnol sleeve. Preloading the outboard by $\pm 80\ \mu\text{m}$ about this minimum point results in n amplitudes reducing to $35\ \mu\text{m}$ pp and $2n$ amplitudes increasing to $15\ \mu\text{m}$ pp. As a matter of good practise the $2n$ values should be kept as low as practicable to avoid any 2/rev surface finish defects and also promote longer spindle and bearing life. For this reason the outboard bearing key was adjusted to this revised alignment position for the remaining engineering and woodmachining tests.

Monitoring the NCDT n and $2n$ values was carried out to investigate the effect of raising the chipbreaker

Table 3 Natural frequencies (r/min)

	Standard	Stage I	Stage II
Structure	4400	–	–
Cutterhead	8900	12 600	18 925

Table 4 Static stiffness measurements ($\text{N}/\mu\text{m}$)

	Standard	Stage I Mod	Stage II Mod
Fence side	105	150	160
Near side	30	55	75

and fitting the jointing device (Fig. 5). This caused $-20\ \mu\text{m}$ (i.e. the outboard bearing moves downwards relative to the spindle) misalignment in the outboard bearing and main spindle. The associated change in spindle frequency n was $+6\ \mu\text{m}$ pp at the NS and $+2\ \mu\text{m}$ pp at the FS. The corresponding change in $2n$ at the NS was $6\ \mu\text{m}$ pp. The FS position showed no detectable change in amplitude at the $2n$ frequency. This observation raises concerns on the use of detachable devices that may inadvertently change the structural characteristics of the machine.

6.1.2 Impulse testing results

The main impulse testing results are shown in Table 3. The outboard bearing housing had a horizontal natural frequency of 4400 r/min which almost coincides with the normal operating speed of 4350 r/min. The cutterhead transverse vibration resonant speed was 8900 r/min. The stage 1 modification to the structure removed any structural resonances in the range of interest i.e. 4000–20 000 r/min. The Stage 1 modification increased the cutterhead transverse vibration resonant speed to 12 600 r/min, indicating that the lack of adequate structural support stiffness (primarily at the NS) on the standard machine had significantly affected the cutterhead transverse vibration speed. The Stage 2 modification increased the cutterhead transverse vibration resonant speed to 18 925 r/min indicating that the Tufnol sleeve clearance also has a significant effect. At this stage, it is important to state that the cutterhead transverse vibration speed must not be near to the desired operating speed. These structural modifications indicate how the speed may be adjusted by careful attention to the mechanical structure and interface element design/manufacture.

6.1.3 Static stiffness results

Table 4 shows the static stiffness results for both FS and NS and the three machine conditions studied. For the standard structure, the radial stiffness at the NS ($30\ \text{N}/\mu\text{m}$) is small in comparison to the FS ($105\ \text{N}/\mu\text{m}$). The addition of the Stage 1 elements increases the NS stiffness significantly to $55\ \text{N}/\mu\text{m}$ and the FS stiffness to $150\ \text{N}/\mu\text{m}$. The addition of the Stage 2 modifications has only a slight effect on the FS stiffness, but increases the NS stiffness by almost 50 per cent to $75\ \text{N}/\mu\text{m}$. This is over twice

Table 5 Sweep test data 1500–5000 r/min μm p-p NCDT NS

	Standard	Stage I Mod	Stage II Mod
'0' imbalance	–4	9	0
675 gm · mm imbalance	3 ^a	23	6

^aActually 30 μm at 4400 r/min resonance

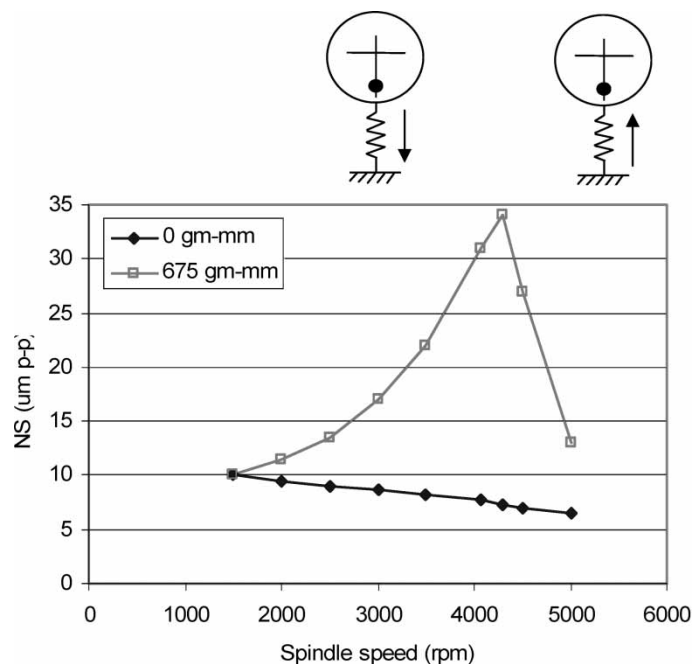
the standard structure NS stiffness and is comparable to the single deep groove rolling element bearing stiffness. This indicates that should further increases in stiffness be sought for the NS position then a double row angular contact arrangement similar to the FS position should be investigated. This would lead to a substantial redesign of both the outboard bearing assembly and the main spindle unit due to the fact that three super precision heavy duty preloaded bearings in line would present considerable manufacturing difficulties. Changing the emphasis of the design to provide equal support at the outboard and fence side positions seems logical. The third (rear) bearing in the main spindle unit could then be made a simple deep groove arrangement to provide power transmission support.

6.1.4 Sweep testing results

Sweep test results are presented for the NS position as these are the more pronounced, generally being two to three times those at the FS position. Sweep tests carried out on the standard structure for the '0' imbalance case are characterized by a steady non-linear increase in structural vibration with spindle speed. This

structural vibration reaches a maximum of 30 μm pp at 4400 r/min and then reduces as the speed increases past the structural resonance. Table 5 shows the change in NCDT values at the NS throughout the speed range for the standard structure and the Stages 1 and 2 modifications. The NS NCDT displacement (Fig. 10) actually reduces in a linear manner as spindle speed increases due to the structural vibration effects. The fact that the standard structure with '0' applied imbalance shows a reduction of 4 μm pp from the static run out value of 10 μm pp is due to the compensatory nature of the structural resonance at 4400 r/min. This observation supports operational practise where certain machines exhibit better performance than others, probably caused by minor changes in operating speed and subtle changes in structural resonant frequency.

For the 675 gm · mm imbalance case, the structural vibration on the standard structure exhibits a pronounced structural resonance at 4400 r/min. This is also evident from the NS NCDT values in Fig. 10. The relative motion between the forcing imbalance vector and the structural vibration are shown. The level of spindle displacement (35 μm pp) measured by the NCDTs at the NS at 4400 r/min is considerably greater than for the '0' imbalance case. The NCDT value reduces quickly past resonance to 3 μm pp greater than the static run out of 10 μm pp. Below resonance, the imbalance vector and vertical displacement vectors are in phase, whereas above resonance, they are in anti-phase. The influence of the resonance increases with imbalance value. With this characteristic it is clear that



Typical vibration response during variable speed operation of the standard test rig.

The system is characterised by a resonance at 4400 rpm. Below this speed the vertical vibration and imbalance vector are in phase. Above this speed the vertical vibration and imbalance vector are 180° out of phase

Fig. 10 Standard structure resonance

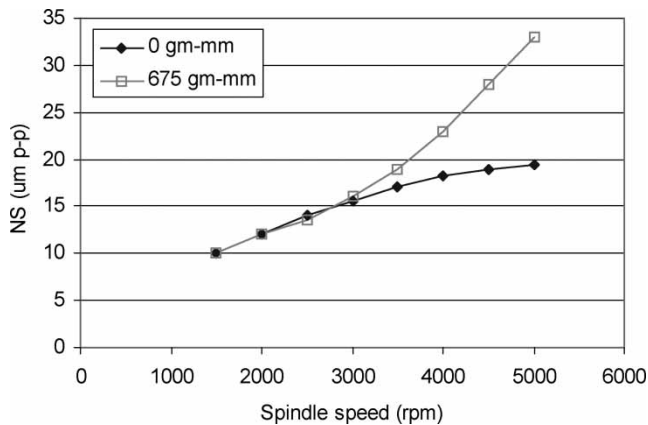


Fig. 11 Imbalance response for Stage 1 structure

jointing and keeping a good quality surface finish would seem highly improbable. Practical experience confirms this.

The Stage 1 modification removes this structural resonance and Table 5 shows the effect on cutterhead run out values through the speed range. The effects of imbalance coupled with rotational speed create a steady non-linear increase in cutterhead run out as speed increases for the '0' imbalance case reaching $9 \mu\text{m pp}$ at 5000 r/min (Fig. 11). The application of the $675 \text{ gm} \cdot \text{mm}$ imbalance creates a corresponding $23 \mu\text{m pp}$ increase. There is no compensatory effect from the structural imbalance, hence, the run out is greater than for the standard structure. In effect, the imbalance vector at the NS is now reacting against the combined stiffness of the spindle/cutterhead and the Tufnol sleeve/outboard bearing compliance.

The addition of the hydrogrip outboard bearing for the Stage 2 modification reduces the sweep speed change to effectively zero for the '0' imbalance case, with a corresponding value of $6 \mu\text{m pp}$ for the $675 \text{ gm} \cdot \text{mm}$ imbalance case (Table 5, Fig. 12).

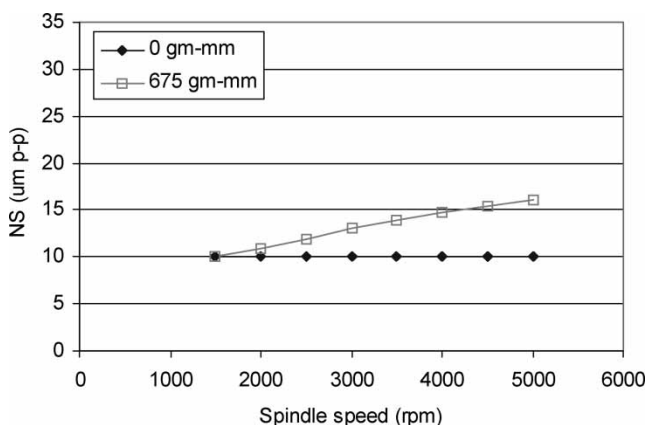


Fig. 12 Imbalance response for Stage 2 structure

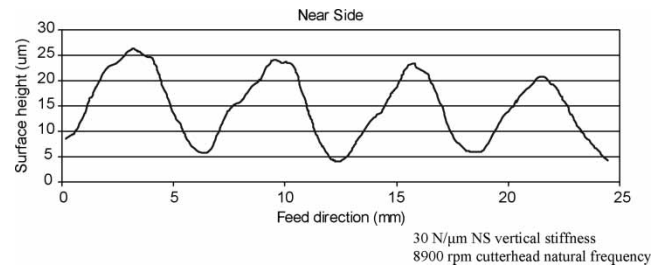


Fig. 13 Standard structure NS surface trace $p = 1.5 \text{ mm}$

These tests show that the standard structure is weak dynamically, in the outboard bearing structure especially. This coupled with the Tufnol sleeve clearance allows considerable orbit change with speed and imbalance effects. By stiffening the structure and removing the outboard bearing support sleeve clearances, a more robust mechanical structure is achieved.

6.2 Woodmachining results

The effects of engineering changes are evaluated via the wood machining tests for the different stages of machine modification. The test rig was subjected to over 50 cutting tests.

6.2.1 Standard structure

The machined timber surface trace in Fig. 13 for the NS is typical for the zero imbalance condition ($<60 \text{ gm} \cdot \text{mm}$) and for a surface wave pitch p of 1.5 mm produced by the standard structure. Table 6 shows typical vibration data during the test. The difference in cutterhead run out at the spindle frequency n at the NS vertical position (i.e. cutting plane) between the jointing and cutting stages is $5 \mu\text{m}$. The static cutter tracking errors are $15 \mu\text{m pp}$ as is the 1/rev surface waviness amplitude in Fig. 13. The periodic marking at four times the wave pitch p is clearly visible from the surface trace.

It is not possible to make a clear analysis of what is happening in this machine operational state because there are so many variables interacting. While a deeper and more extensive focused investigation on this case could be done, it was deemed pointless since the test work had revealed that serious dynamic structural flaws existed and needed to be resolved. The phased improvement through Stages 1 and 2 modifications was, therefore, pursued. Speculatively, the most likely explanation of the standard structure observations is that the structural vibration makes the jointer move relative to the cutterhead and thus dresses a 1/rev shape onto the cutters. This is complicated

Table 6 Experimental results – normal imbalance

Cutterhead NF (r/min)	Standard structure		Stage 1 modification		Stage 2 modification	
	8900		12 600		18 925	
Parameter						
Position	FS	NS	FS	NS	FS	NS
Radial stiffness (N/ μm)	105	30	150	55	160	75
NCDT joint-cutting (μm)	3	5	0	2	0	0
Cutter tracking errors (μm)	7	15	1	10	0	0
Surface 1/rev amplitude (μm)	6	15	3	6	1	2

by the fact that the cutterhead is also vibrating in the vertical plane at the cutting point, so a combined effect results. The application of $675 \text{ gm} \cdot \text{mm}$ imbalance at any cutter position at the NS results in displacement values approximately twice as large as for the zero imbalance condition. The $15 \mu\text{m}$ pp 1/rev amplitude on the NS trace in Fig. 13 is typical of the poor quality achieved on this type of production machine. Even though a machine weighs 6 tonnes, comprising of cast iron and high grade steel, the fundamental design flaws that produce the structural resonance coupled with the detailed weaknesses associated with slide friction and Tufnol bush clearances lead one to understand that initial superficial appearances can hide a host of weaknesses at the micrometre level.

6.2.2 Stage 1 modification

A typical surface trace result for the Stage 1 modification is shown in Fig. 14. The same wave pitch of $p = 1.5 \text{ mm}$ is maintained. The corresponding test results summary is in Table 6. The NCDT change at the NS cutting point between jointing and cutting has reduced to $2 \mu\text{m}$ pp. This is less than half that for the standard structure. Significantly, the level of $2 \mu\text{m}$ shows that higher surface qualities should result. However, the static cutter tracking errors after jointing at the NS are $10 \mu\text{m}$ pp compared to $1 \mu\text{m}$ pp at the FS. This suggests that the cutterhead is adopting a slightly bent shape due to the dynamic imbalance effects initiated by the small residual

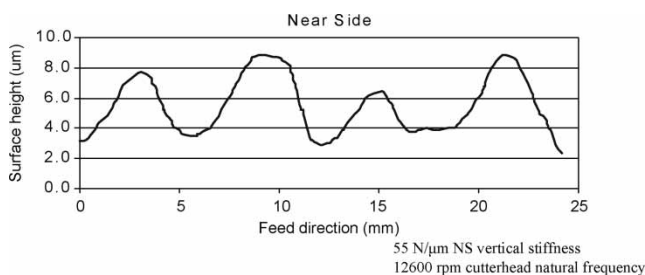


Fig. 14 Stage 2 modification NS surface trace $p = 1.5 \text{ mm}$

imbalance and thus deflecting across the clearance between the spindle and the NS Tufnol sleeve. Significantly, in Fig. 14, the surface waviness trace at the NS exhibits a $6 \mu\text{m}$ pp 1/rev effect and while this does not compare well with the change between jointing and cutting at the NS of $2 \mu\text{m}$ pp, it does illustrate the level of improvement achieved when compared with the $15 \mu\text{m}$ pp of the surface machined by the standard structure.

6.2.3 Stage 2 modification

A typical surface trace result for the Stage 2 modification is shown in Fig. 15. The same wave pitch of $p = 1.5 \text{ mm}$ is maintained. The corresponding test results summary is in Table 6. There is no measurable difference in the cutterhead orbit between jointing and cutting and similarly no measurable static cutter tracking errors as shown in Table 6. The measured surface waviness is further improved to the point where the limitations of the WRI are reached. Even with the use of a roller stylus, the grain effects of the timber are starting to distort the higher surface quality waveform as seen in the NS trace in Fig. 15. The achieved surface waviness is $2 \mu\text{m}$ pp compared to $15 \mu\text{m}$ pp on the standard structure.

When a large ($675 \text{ gm} \cdot \text{mm}$) imbalance is applied at the NS as a test of robustness, there is an increase in 1/rev waviness on the machined timber surface for the standard structure to $30 \mu\text{m}$ pp, while the same test on the Stage 2 structure results in a 1/rev

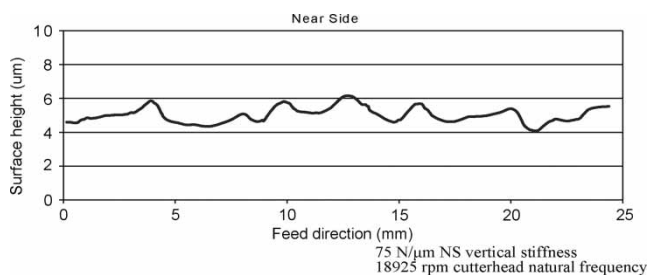


Fig. 15 Stage 2 modification NS surface trace $p = 1.5 \text{ mm}$

waviness of $3 \mu\text{m pp}$. The Stage 2 arrangement is not only capable of producing superior surface quality but will also achieve this in a robust manner leading to greater consistency in machine operation. This in turn will increase operator confidence, reduce machine downtime, and generate greater output in a more efficient manner.

7 DISCUSSION

The test results achieved in this work have shown that it is possible to make modifications to a wood-working machine tool structure in stages and quantify the effects of these changes both in terms of measured surface waviness quality on the machined timber samples as well as key engineering parameters at the heart of the machining process. Support stiffness in the vertical direction for a horizontal spindle unit has been shown to be a major factor in achieving high quality surfaces. The standard structure was sufficiently weak dynamically, that the raising of the chipbreaker and attachment of the jointing device were sufficient to change the NS spindle orbit by $6 \mu\text{m pp}$. This is sufficient to cause a significant surface defect. Misalignment due to main spindle and outboard bearings being on separate slideways linked by dual rise and fall screws can cause significant changes in spindle orbit at both the spindle rotational frequency and the first harmonic. Orbit change between jointing and cutting was thought to be an issue, but a tight correlation could not be observed. It can be said that as the structural integrity of the machine increases, the measured orbit change between jointing and cutting does reduce. However there is no correlation to measure static cutter run outs – this is a useful conclusion because this is one way the wood machining trade believes they can quantify if a good surface is likely. The answer seems to be that the machine must possess a high radial stiffness ideally $100 \text{ N}/\mu\text{m}$ and no radial clearances in either sleeves or bearings greater than $3 \mu\text{m}$.

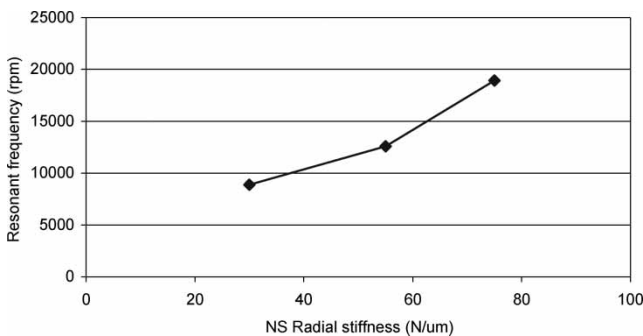


Fig. 16 Radial stiffness of cutterhead support

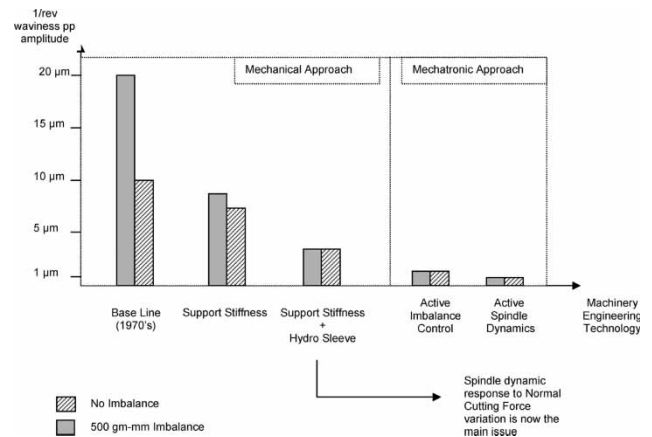


Fig. 17 Technology road map for future machine design

Additional work to observe joint land width on cutting forces and spindle run out at 1/rev and the cutter passing frequency should yield information on the influence of these parameters on surface waviness quality. It is interesting to see how the cutterhead natural frequency increases with the NS static stiffness as shown in Fig. 16. The proximity of the knife passing frequency at for example 4500 r/min with four cutters shows the potential problem with mechanically stiff structures. This suggests variations in joint land width and hence normal cutting force may couple with resonance energy to cause wave mark variation. This is the subject of further research.

Also the subject of current and future research is the idea that a purely mechanical solution to improve waviness (and also texture) has reached a natural limit (Fig. 17). The potential of active systems should be explored to sense the machined surface quality and actively control the cutterhead displacement to always achieve the desired result at the desired feed speed. Such systems have the potential to revolutionize the dry machining of materials such as wood and plastic. Initial simulation work [12] has shown this to be viable and investigations using a smart spindle unit will be reported in a future paper.

8 CONCLUSIONS

Structural stiffness is the first requirement in achieving good quality machined timber surfaces. Structural mass alone is of no use. The detailed structural integrity across location sleeves is sufficiently low to cause poor machined surface quality. The combined result of good structural stiffness and integral hydraulically contracting location sleeves can produce combined stiffness of the order of $100 \text{ N}/\mu\text{m}$. This is sufficient to achieve good quality

surfaces where the 1/rev amplitude is less than 2 μm at a wave pitch of 1.5 mm. The higher quality surfaces with a wave pitch less than 1.5 mm are only achievable under particular unknown circumstances and should be the subject of further research.

REFERENCES

- 1 **Jackson, M. R., Parkin, R. M., and Brown, N.** Waves on wood. *Proc. Instn Mech. Engrs, Part B: J. Engineering Manufacture*, 2002, **216**, 475–497. ISSN 09 54-4054.
- 2 **Petter, J. C.** Development work on wood planers. *Forest Prod. Res. Soc.*, 1954, **543**, 1–3.
- 3 **Mori, M. and Hoshi, T.** Studies on surfacing of wood with planer (I). *Bull. Gov. Forest Exp. Station*, 1964, **160**, 1–24.
- 4 **Mori, M. and Hoshi, T.** Studies on surfacing of wood with planer (II). *Bull. Gov. Forest Exp. Station*, 1964, **163**, 1–18.
- 5 **Mori, M.** Studies on surfacing of wood with planer (IV). *Bull. Gov. Forest Exp. Station*, 1964, **163**, 1–13.
- 6 **Koch, P.** An analysis of the lumber planing process: part I. *Forest Prod. J.*, 1955, pp. 255–264.
- 7 **Koch, P.** An analysis of the lumber planing process: part II. *Forest Prod. J.*, 1956, **6**(10), pp. 393–402.
- 8 **Kivimaa, E.** *Cutting forces in woodworking*. PhD Thesis, University of Helsinki, 1950.
- 9 **Jackson, M. R. and Buttery, T. C.** Some effects of machine parameters on cutting forces and surface geometry in rotary planing of wood and polymers. Second Joint Polytechnics Symposium on *Manufacturing engineering*, Lanchester Polytechnic, June 1979, pp. 196–201.
- 10 **Jackson, M. R.** *Some effects of machine characteristics on the surface quality of planed and spindle moulded wooden products*. PhD Thesis, Leicester Polytechnic, 1986.
- 11 **Heisel, U. and Krondorfer, H.** Surface method for vibration analysis in peripheral milling of solid wood, Proceeding of the 12th International Wood Machining Seminar, Kyoto, Japan, 1995, pp. 115–125.
- 12 **Hynek, P., Jackson, M., and Parkin, R., and Brown, N.** Improving wood surface form by modification of the rotary machining process. *Proc. Inst. Mech. Engrs, Part B: J. Engineering Manufacture*, 2004, **218**(8), 875–887.

APPENDIX

Notation

$a_{1/\text{rev}}$	interfering radial displacement every cutterhead revolutions (mm)
h	depth of cutter mark (mm)
L	length of cutter engagement path with timber (mm)
n	cutterhead rotational velocity (r/min)
N	number of cutters producing a finishing surface wave
p	cutter wave pitch (mm)
R	cutterhead radius (mm)
R_w	wave width ratio
V	workpiece feed velocity (m/min)
W_n	width of surface wave n (mm)
α	cutter rake angle ($^\circ$)
β	cutter sharpness angle ($^\circ$)
γ	cutter clearance angle ($^\circ$)